Island Arc (2008) **17,** 172–182

Research Article

Mantle heterogeneity beneath the Antarctic–Phoenix Ridge off Antarctic Peninsula

SUNG-HI CHOI, WON-HIE CHOE AND JONG-IK LEE*

Korea Polar Research Institute, Songdo Techno Park 7-50, Songdo-dong, Yeonsu-gu, Incheon 406-840, Korea (jilee@kopri.re.kr)

Abstract We determined the Sr, Nd and Pb isotopic compositions of basalts recovered from the Antarctic–Phoenix Ridge (APR), a fossil spreading center in the Drake Passage, Antarctic Ocean, in order to understand the nature of the subridge mantle source. There are no known hotspots in close proximity to the site. We observe that small-scale isotopic heterogeneity exists at a shallow level in the subaxial mantle of the APR. Enriched (E-type) mid-ocean ridge basalts (MORB) coexist with normal (N-type) MORB in this region. The E-type basalts are: (i) relatively young compared to the N-type samples; (ii) were erupted after the extinction of the APR; and (iii) have been generated by low-degree partial melting of an enriched mantle source. Extinction of the APR likely caused the extent of partial melting in this region to decrease. We interpret that the geochemically enriched materials dispersed in the ambient depleted mantle were the first fraction to melt to form the E-type MORB.

Key words: Antarctic–Phoenix Ridge, E-type MORB, heterogeneity, Sr–Nd–Pb isotopes.

INTRODUCTION

Mid-ocean ridge basalts (MORB) are dominated by tholeiites that are depleted in incompatible trace elements, and as a whole display small geochemical variations compared with basalts from other tectonic settings (e.g. Melson *et al.* 1976). The oceanic upper mantle source of MORB has thus been designated as a depleted mantle (Zindler & Hart 1986), and is considered to be a homogeneous mantle source reservoir. However, incompatible element enriched basalts (E-type MORB) resembling those from oceanic islands are commonly reported at all ridges and in all ocean basins (e.g. Niu *et al.* 1999; Donnelly *et al.* 2004; Debaille *et al.* 2006). These observations suggest that complete homogeneity in the oceanic upper mantle is not tenable. The origin of E-type MORB has been generally invoked to be due to plume–ridge interactions based on compositional variations of MORB toward on- and near-ridge hotspots (e.g. Iceland, the Azores, and Bouvet) (Sun *et al.* 1975; Schilling *et al.* 1983; Le Roex *et al.* 1992; Dosso *et al.* 1993; Taylor *et al.* 1997). However, the occurrence of E-type MORB far from hotspots (Niu *et al.* 1999; Donnelly *et al.* 2004) is not readily explained by the interaction of enriched plumes from the deep mantle with the dominantly depleted mid-ocean ridge basalts (N-type MORB) mantle source.

The Antarctic–Phoenix Ridge (APR), the last remnant of the once-extensive spreading center in the Drake Passage between South America and Antarctica, is remote from the influence of hotspots (Fig. 1). The APR lavas have recently been studied for their major and trace element characteristics (Choe *et al.* 2007); N-type and E-type MORB coexist in this area. The APR is thus an excellent place to examine the intrinsic isotopic heterogeneity in the oceanic upper mantle. Here, we present Sr–Nd–Pb isotopic compositions of 17 axial MORB samples from the APR. The samples are a subset of those previously studied by Choe *et al.* (2007). Our data provide insights into the nature and distribution of heterogeneity in the upper mantle source of MORB.

*Correspondence.

Received 4 June 2007; accepted for publication 5 October 2007.

doi:10.1111/j.1440-1738.2007.00609.x

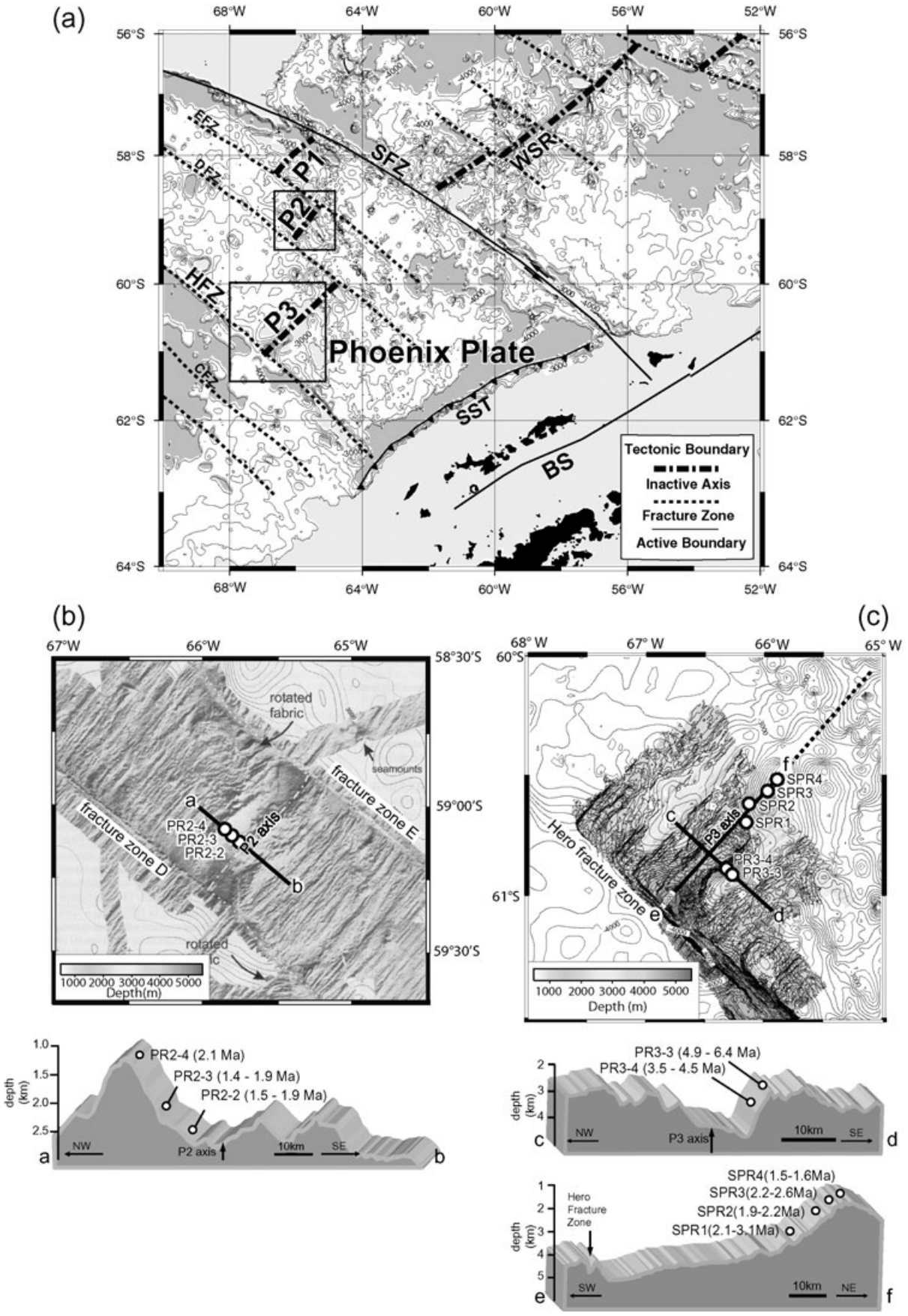

Fig. 1 (a) Tectonic boundary map over the bathymetry using satellite altimetry in the Drake Passage (modified from Smith & Sandwell 1994). Contours are depths in meters below sea level. Abbreviations: P1, P2, P3, Antarctic–Phoenix Ridges; SFZ, Shackleton Fracture Zone; HFZ, Hero Fracture Zone; SST, South Shetland Trench; WSR, West Scotia Ridge; BS, Bransfield Strait; DFZ, D Fracture Zone; EFZ, E Fracture Zone. (b, c) Bathymetry and depth profile of the P2 and P3 segments, respectively, modified from Livermore *et al.* (2000). Circles are sample locations with K–Ar whole-rock ages (Choe *et al.* 2005).

GEOLOGICAL SETTING AND SAMPLING

The APR consists of three inactive segments (P1, P2, and P3; Fig. 1a) between the Shackleton and Hero Fracture Zones. Spreading of the APR slowed abruptly at the time of magnetic chron C4A (*ca* 7.8 Ma), probably as a result of extinction of the West Scotia Ridge (Fig. 1a), and became extinct at chron C2A (*ca* 3.3 Ma) (Larter & Barker 1991; Livermore *et al.* 2000). Extinction might have been simultaneous on all three remaining segments of the ridge, and synchronous with the final ridge–trench collision to the southwest of the Hero Fracture Zone (Livermore *et al.* 2000). Estimated spreading rates were from >30 mm/y prior to chron C4A to 13 mm/y just before extinction (Livermore *et al.* 2000).

The Antarctic Circumpolar Current in the Drake Passage is strong enough to prevent thick sediment accumulation. The fossil spreading centers of the APR are thus uniquely exposed for bathymetric mapping and dredging. During the 1999–2000 austral summer season, half of the P3 segment was mapped using a SEABEAM 2000 multibeam echo sounder on the Korean research vessel R/V *Onnuri*. Fresh lavas from P2 and P3 segments have been dredged during the 2000–01 and 2002–03 summer cruises onboard R/V *Yuzhmorgeologiya*.

The off-axis morphology of the P2 segment is generally comparable to that of fast- or intermediate-spreading ridges dominated by linear, axis-parallel, magmatic ridges and straight, sharply defined fracture zones. However, its axial region is characterized by anomalous high-relief paired ridges (Fig. 1b). The samples named as PR2- have been collected from the inner wall of the northwest flank. The K–Ar whole-rock ages for the basalts range 2.1–1.4 Ma (Choe *et al.* 2005).

The near-axis morphology of the P3 segment is also characterized by high relief (Fig. 1c). A prominent seamount, rising 2500 m from the axial valley floor, is present in the center of the segment. The samples named as SPR have been collected from the seamount, and dated as 3.1–1.4 Ma (Choe *et al.* 2005). The axial seamount is flanked by two great ridges to the southwest. The samples named as PR3- have been collected from the southeastern ridge. The K–Ar ages for the basalts are from 3.5 to 6.4 Ma (Choe *et al.* 2005).

Major and trace element chemistry of the PR3- basalts (Choe *et al.* 2007) are those of N-type MORB, whereas those for the axial seamount (SPR) and PR2- basalts are those of E-type MORB. That is, the PR3- basalts are low-K tholeiites, and have lower Zr/Y (<4) and slightly light rare earth element (LREE)-depleted patterns on the chondrite-normalized REE plot. Also, the SPR and PR2- samples are (medium-K) mildly alkaline basalts, and have higher Zr/Y (5–12) and strongly LREE-enriched patterns. We note that the E-type basalts are relatively younger than the N-type samples, and were erupted after the proposed extinction of the APR.

ANALYTICAL PROCEDURES

The samples studied are fresh, olivine- or olivine–plagioclase-phyric basalts. The samples were crushed to approximately mm-size fragments, ultrasonically cleaned (mili-Q), and phenocryst-free fragments handpicked. Sr, Nd and Pb isotope analyses, including chemical separation and measurements on a Finnigan MAT-262 thermal ionization mass spectrometer, were performed at the Laboratory for Radiogenic Isotope Geochemistry, Institute of Geology and Geophysics, Chinese Academy of Sciences, Beijing, China. Ratios of $^{87}Sr/^{86}Sr$ and $^{143}Nd/^{144}Nd$ were corrected for instrumental mass fractionation by normalizing to $^{86}Sr/^{88}Sr = 0.1194$ and $^{146}Nd/^{144}Nd = 0.7219$, respectively. Replicate analyses of NIST SRM-987 and La Jolla standards gave $^{87}Sr/^{86}Sr = 0.710208 \pm 9$ ($N = 10$, 2σ) and $^{143}Nd/^{144}Nd = 0.511826 \pm 8$ ($N = 12$, 2σ), respectively. Measured Pb isotopic ratios were corrected for instrumental mass fractionation of 0.1% per atomic mass unit by reference to replicate analyses of the NIST SRM-981. Total blanks averaged 0.2 ng for Sr, 0.05 ng for Nd, and 0.05 ng for Pb. The results are given in Table 1, along with isotope dilution measurements for Rb, Sr, Sm, and Nd.

Table 1 Sr–Nd–Pb isotopic compositions for basalts from the Antarctic–Phoenix Ridge in the Drake Passage, Antarctic Ocean

Sample No.	Age (Ma)†	Mg#‡	F (%)	$(La/Sm)_N$‡	K_2O/TiO_2‡	$(Sm/Yb)_N$‡	[Rb] ppm	[Sr] ppm	$^{87}Rb/^{86}Sr$	$^{87}Sr/^{86}Sr \pm 2\sigma$	[Sm] ppm	[Nd] ppm	$^{147}Sm/^{144}Nd$	$^{143}Nd/^{144}Nd \pm 2\sigma$	ε_{Nd}	$^{206}Pb/^{204}Pb$	$^{207}Pb/^{204}Pb$	$^{208}Pb/^{204}Pb$
Segment P2																		
PR2-2-1	1.5	52.5	14.4	2.28	0.65	2.39	20.8	277	0.2159	0.703318 ± 14	7.5	31.7	0.1426	0.512944 ± 11	6.0	18.90	15.59	38.62
PR2-2-2	1.6	53.2	12.4	3.04	0.74	1.95	29.9	279	0.3123	0.703298 ± 17	8.8	38.6	0.1380	0.512954 ± 11	6.2	18.95	15.63	38.77
PR2-3-2	1.9	47.1	14.8	2.81	0.53	1.90	22.9	302	0.2178	0.703225 ± 11	8.0	34.1	0.1414	0.512942 ± 11	5.9	18.89	15.56	38.54
PR2-3-3	1.8	46.8	14.6	2.80	0.59	1.91	23.6	296	0.2283	0.703232 ± 11	8.3	35.7	0.1412	0.512954 ± 12	6.2	18.81	15.60	38.62
PR2-4-1	2.1	52.5	16.8	2.53	0.44	1.80	15.1	306	0.1414	0.703279 ± 10	6.0	24.1	0.1503	0.512914 ± 13	5.4	18.90	15.58	38.60
Segment P3																		
SPR1-2	2.1	66.5	14.0	2.23	0.40	1.82	9.3	266	0.1008	0.703079 ± 12	4.9	19.9	0.1488	0.512963 ± 12	6.3	19.06	15.64	38.88
SPR1-3	2.3	66.8	13.9	2.22	0.45	1.85	49.3	266	0.5393	0.703212 ± 12	4.8	19.4	0.1482	0.512964 ± 11	6.4	19.03	15.62	38.78
SPR2-2	2.0	61.8	12.9	3.06	0.68	2.09	18.1	349	0.1498	0.702953 ± 11	5.4	24.5	0.1345	0.512967 ± 12	6.4	19.03	15.58	38.64
SPR2-3	2.2	63.0	12.3	2.99	0.65	2.09	14.5	347	0.1206	0.702951 ± 10	5.3	24.0	0.1349	0.512990 ± 12	6.9	19.02	15.63	38.79
SPR3-1	2.5	54.5	14.8	2.44	0.46	1.63	21.5	268	0.2315	0.702586 ± 10	5.0	20.0	0.1506	0.512984 ± 13	6.7	18.97	15.53	38.30
SPR3-2	2.2	53.8	15.3	2.51	0.41	1.65	16.0	254	0.1831	0.702570 ± 11	3.9	15.9	0.1497	0.512983 ± 13	6.7	18.83	15.58	38.46
SPR3-4	2.6	55.9	14.6	2.24	0.40	1.53	15.0	255	0.1698	0.702581 ± 11	3.2	11.8	0.1625	0.512992 ± 12	6.9	18.92	15.55	38.34
SPR4-1	1.5	58.5	11.7	3.42	0.65	1.83	23.9	368	0.1879	0.702745 ± 12	2.5	12.5	0.1229	0.512972 ± 11	6.5	19.05	15.57	38.52
SPR4-6	1.5	49.0	14.7	2.71	0.63	1.80	22.0	385	0.1649	0.702732 ± 13	3.1	12.4	0.1495	0.512965 ± 11	6.4	19.03	15.58	38.46
PR3-3-1	6.4	62.1	17.7	0.74	0.21	1.31	7.1	173	0.1183	0.702591 ± 12	3.5	10.6	0.2000	0.513110 ± 12	9.2	18.52	15.53	38.00
PR3-3-2	4.9	62.6	17.5	0.73	0.24	1.35	7.3	177	0.1208	0.702686 ± 11	3.5	10.4	0.2022	0.513096 ± 12	8.9	18.51	15.54	38.05
PR3-4-2	3.5	62.7	17.1	0.76	0.14	1.18	2.5	147	0.0479	0.702809 ± 10	3.0	8.6	0.2091	0.513113 ± 12	9.3	18.57	15.52	38.03

†Data from Choe *et al.* (2005).
‡Data from Choe *et al.* (2007).
Mg# = 100 Mg/(Mg + Fe^{2+}) with 10% total Fe as Fe^{3+}.
F (%) = percentage of partial melting as estimated from fractionation-adjusted major element abundances following Niu and Batiza (1991).

RESULTS

Ratios of $^{87}Sr/^{86}Sr$ for the E-type PR2- and SPR basalts span a wide range (0.702570–0.703318), whereas those for the N-type PR3- samples span a relatively limited range (0.702591–0.702809) that overlaps with the less radiogenic end of the E-type basalts (Table 1; Fig. 2). However, the Nd and Pb isotopic compositions significantly distinguish the different sample groups. The E-type basalts are characterized by less radiogenic Nd and more radiogenic Pb isotopic compositions ($^{143}Nd/^{144}Nd$ = 0.512914–0.512992, ε_{Nd} = +5.4 to +6.9, $^{206}Pb/^{204}Pb$ = 18.81–19.06, $^{207}Pb/^{204}Pb$ = 15.53–15.64, and $^{208}Pb/^{204}Pb$ = 38.30–38.88) than the N-type basalts ($^{143}Nd/^{144}Nd$ = 0.513096–0.513113, ε_{Nd} = +8.9 to +9.3, $^{206}Pb/^{204}Pb$ = 18.51–18.57, $^{207}Pb/^{204}Pb$ = 15.52–15.54, and $^{208}Pb/^{204}Pb$ = 38.00–38.05). On the $^{87}Sr/^{86}Sr$ *vs* $^{143}Nd/^{144}Nd$ isotopic correlation diagram (Fig. 2a), the N-type basalts plot within the field of Pacific/Atlantic MORB, meanwhile the E-type samples plot off the field, showing a radiogenically enriched Indian MORB-like isotopic signature. Notably, well-separated bimodal Pb isotope ratios, with high values for E-type and low values for N-type basalts, are shown in Figure 2b,c. In the $^{206}Pb/^{204}Pb$ *vs* $^{208}Pb/^{204}Pb$ space (Fig. 2b), all of the APR basalts plot in the Pacific/Atlantic MORB field. However, some of E-type basalts display more radiogenic $^{207}Pb/^{204}Pb$ ratios than the Indian MORB at a given $^{206}Pb/^{204}Pb$ (Fig. 2c).

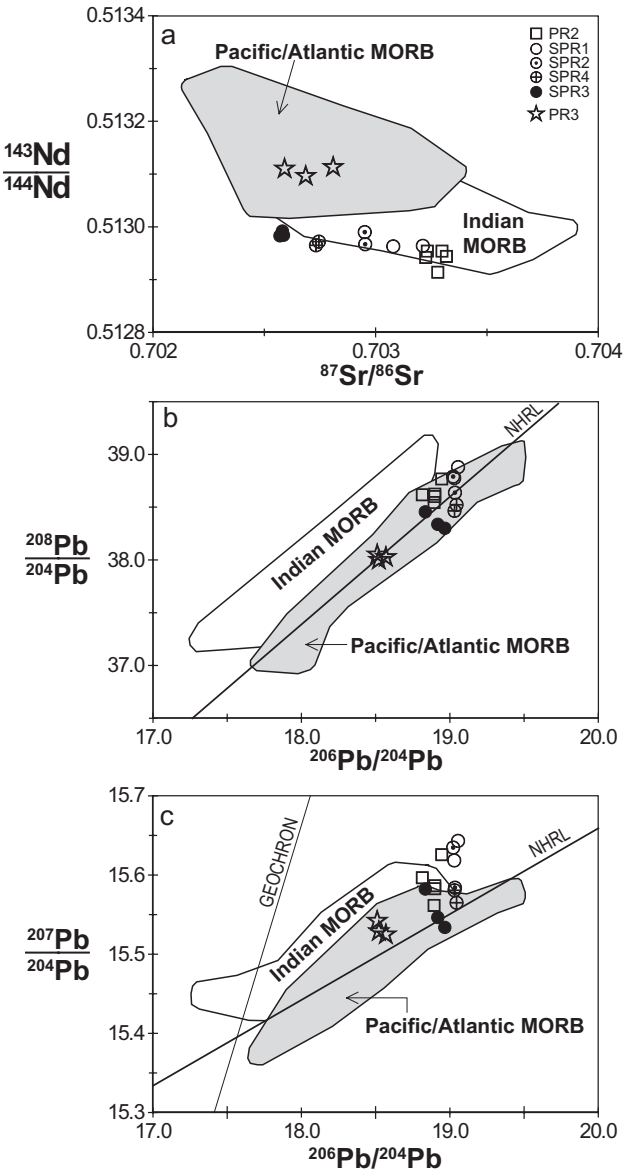

Fig. 2 Sr, Nd and Pb isotopic compositions of the basalts from the Antarctic–Phoenix Ridge. Errors (2 σ) are within the size of the symbol on the plot. MORB, mid-ocean ridge basalts; NHRL, Northern Hemisphere Reference Line of Hart (1984). Data sources for the MORB fields are White and Hofmann (1982), Ito *et al.* (1987), White *et al.* (1987), Mahoney *et al.* (1989; 1992; 1994), Bach *et al.* (1994), Salters and White (1998), Niu *et al.* (1999) and Chauvel and Blichert-Toft (2001).

DISCUSSION

CRUSTAL CONTAMINATION

The basalts studied range from relatively unfractionated (Mg# = 66.8, MgO = 8.6 wt%) to moderately evolved (Mg# = 46.8, MgO = 4.3 wt%) (Table 1; Choe *et al.* 2007), most probably reflecting variable extents of low-pressure fractional crystallization and crustal assimilation. In order to decipher the nature of the mantle source based on the isotopic compositions of the basalts, the assimilation and fractional crystallization effects should be first evaluated. The variation of isotopic compositions of the APR basalts with respect to Mg# (= 100 Mg/[Mg + Fe^{2+}] with 10% total Fe as Fe^{3+}) is shown in Figure 3a–e. The E-type axial seamount basalts (SPR1, 2, and 4) exhibit relatively coherent isotopic compositional variations with respect to Mg#. The Sr and Pb isotopic ratios generally decrease with decreasing Mg#, although the $^{143}Nd/^{144}Nd$ ratios do not show a recognizable variation. The E-type PR2- basalts show similar trends on the plots. In general, the evolved E-type basalts (e.g. samples SPR4-) plot closer to the Pacific/Atlantic MORB fields on the various isotopic correlation diagrams (Fig. 2a–c), whereas the more primitive samples (e.g. samples SPR1) plot further away. Such correlations between isotopic compositions and Mg# indicate that crustal contamination by wall rocks consisting of N-type MORB with less

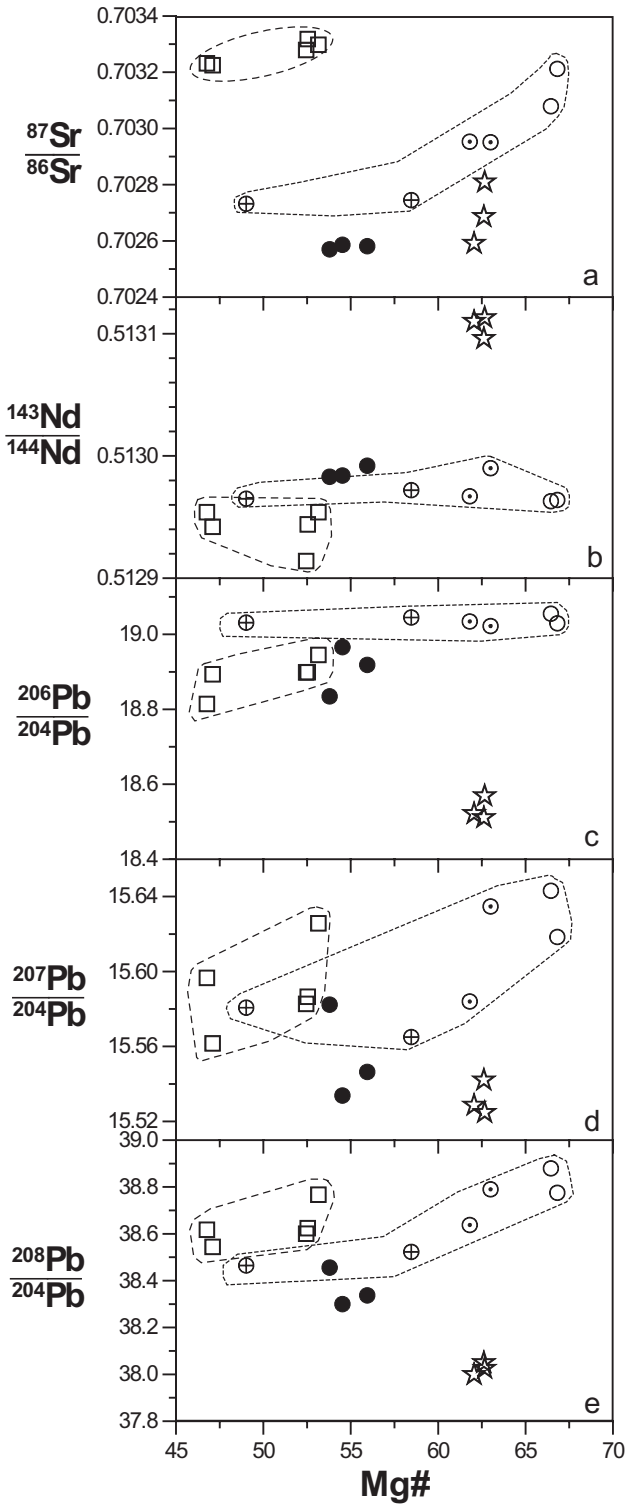

Fig. 3 Variation of isotopic compositions with respect to Mg# in basalts from the Antarctic–Phoenix Ridge. Mg# = 100 Mg/(Mg + Fe^{2+}) with 10% total Fe as Fe^{3+}. Errors (2 σ) are within the size of the symbol on the plot. Symbols as in Figure 2.

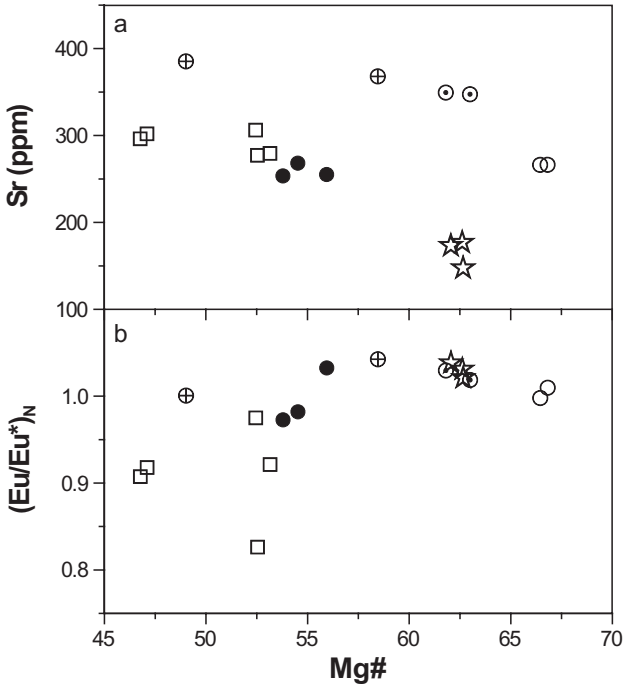

Fig. 4 (a) Sr (ppm), and (b) Eu/Eu* ratio with respect to Mg# in basalts from the Antarctic–Phoenix Ridge. Eu* is calculated as $([Sm]_N + [Gd]_N)/2$, normalized to the composition of chondritic meteorites (Sun & McDonough 1989). Mg# = 100 Mg/(Mg + Fe^{2+}) with 10% total Fe as Fe^{3+}. Errors (2 σ) are within the size of the symbol on the plot. Symbols as in Figure 2.

radiogenic Sr and Pb isotopes than E-type MORB, might be an important process contributing to the isotopic composition of the evolved E-type APR basalts. Therefore, we will use the data only for the relatively primitive SPR1 and PR3- basalts as probes for the nature of the upper mantle source beneath the APR (see below).

It is noteworthy that the SPR3 basalts do not lie along the trend defined by other axial seamount basalts (SPR 1, 2, and 4) in Figure 3a–e. The samples are plagioclase-phyric. In order to evaluate the possible plagioclase fractional crystallization effect, we plotted Sr concentration and Eu/Eu* ratio as a function of Mg# in Figure 4a,b, where Eu* is the average of chondrite-normalized Sm and Gd concentrations. The SPR3 samples do not show any significant Eu anomalies. Therefore, the off-set of Sr concentration level toward lower values at a given Mg# by SPR3 can not be accounted for by plagioclase fractional crystallization. This observation, along with deviation from the trends in isotopic plots (Fig. 3a–e), indicates that these lavas were derived from compositionally different parental magmas. That is, the axial seamount was not likely to have been built by only one batch of melt.

MANTLE SOURCE HETEROGENEITY

In order to reveal the nature of mantle source, it is also necessary to know the chemical systematics of

the incompatible trace elements in the magma source. The ratio of light- to heavy-rare earth elements normalized to the chondritic values (i.e. $[La/Sm]_N$), has been considered as a good indicator of enrichment of the source (e.g. Batiza & Vanko 1984; Hékinian *et al.* 1989; Debaille *et al.* 2006), with greater values corresponding to more enriched mantle. The E-type APR basalts are characterized by elevated $(La/Sm)_N$ ratios, ranging 2.2–3.4, relative to the N-type samples which have an average value of approximately 0.7 (Table 1). In Figure 5a–d, we compared the Sr–Nd–Pb isotopic compositions with $(La/Sm)_N$ ratios. Relatively primitive basalts (SPR- and PR3-) were used in this approach, as discussed above. It is clear that the highly incompatible element ratios are strongly coupled with the isotopic compositions. The $(La/Sm)_N$ ratios are positively correlated with the Sr and Pb isotopic compositions, and negatively with the Nd isotopic ratios. Shen and Forsyth (1995) argued that K_2O/TiO_2 can serve as an indicator to separate E-type MORB from N-type MORB, similar to La/Sm. In Figure 5e, a systematic change in the K_2O/TiO_2 ratios of the APR

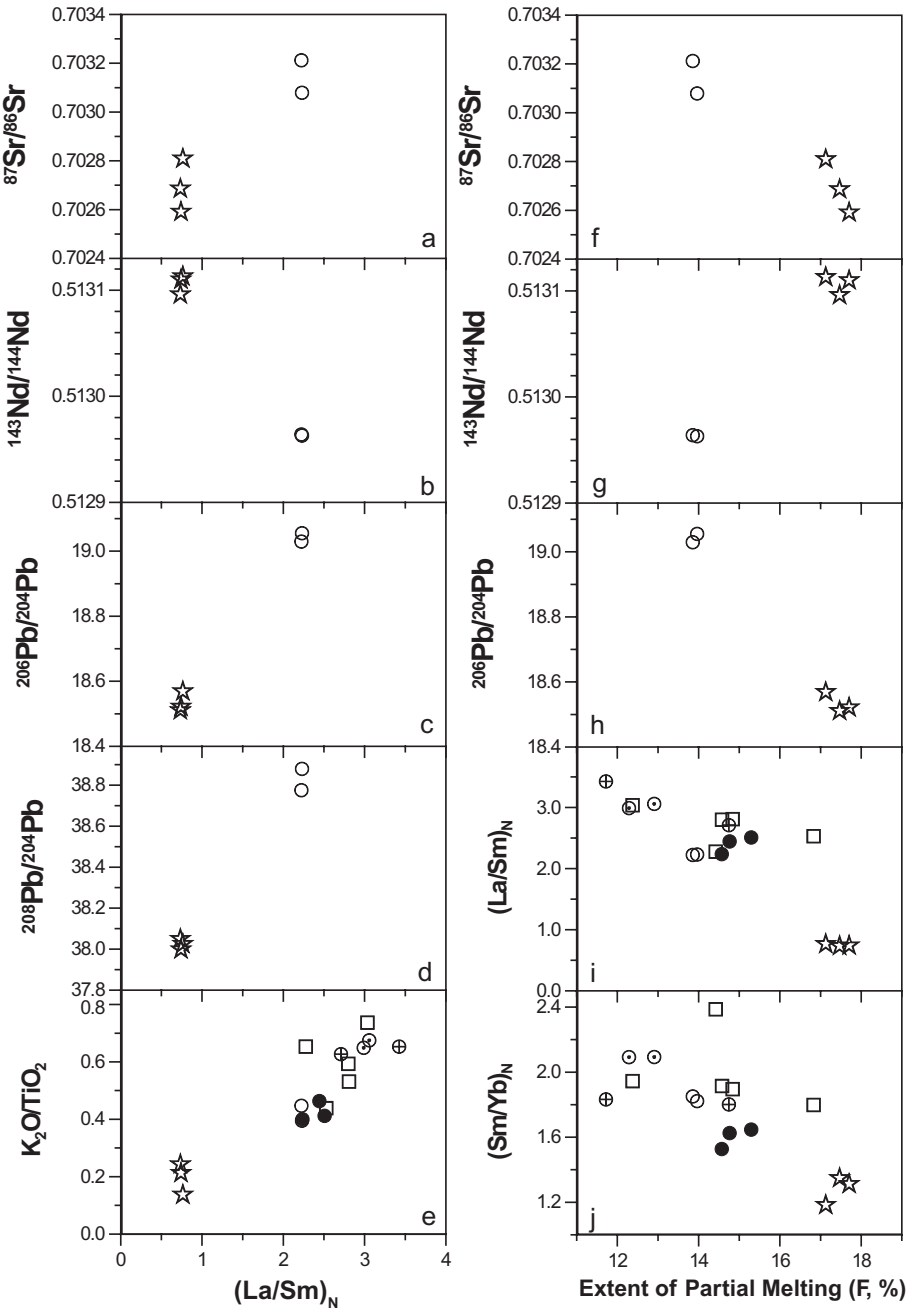

Fig. 5 (a–e) Isotopic systematics and incompatible element ratios *vs* $(La/Sm)_N$, normalized to the composition of chondritic meteorites (Sun & McDonough 1989), and (f–j) extent of partial melting. Symbols as in Figure 2.

basalts with the $(La/Sm)_N$ ratios can be seen, independently supporting the notion that the mantle source beneath the APR is heterogeneous with respect to incompatible trace elements and Sr–Nd–Pb isotopic compositions. The most important implication is that these correlations between incompatible trace element and isotopic ratios reveal the existence of two end-member components: one enriched component with more radiogenic Sr and Pb and less radiogenic Nd isotopic ratios, and a depleted end-member.

In order to evaluate whether the processes of mantle melting are related with the mantle source heterogeneity, we estimated the extent of melting following the method of Niu and Batiza (1991) based on major element compositions, after normalization to a constant MgO content of 8 wt% to correct for crustal-level crystal fractionation. The correction coefficients by Niu *et al.* (1996) were used in the calculation. The determined extent of melting (F) of the APR basalts varies from 12 to 18%. Values are given in Table 1 and illustrated in Figure 5f–i with respect to isotopic compositions and incompatible trace element ratios. It is clear that the E-type basalts, having more radiogenic Sr and Pb and less radiogenic Nd isotopic as well as elevated $(La/Sm)_N$ ratios, represent a relatively small degree of melting in comparison with the N-type basalts. For an independent evaluation of the estimation of extent of melting, we plot the $(Sm/Yb)_N$ ratios of the APR basalts as a function of F determined from major element chemistry in Figure 5j. Since $(Sm/Yb)_N$ is not sensitive to olivine- and plagioclase-dominated low-pressure fractional crystallization processes (Ellam 1992), it may reflect primarily the variation in melting processes and source compositions, with higher $(Sm/Yb)_N$ ratio corresponding to a lower extent of partial melting. The $(Sm/Yb)_N$ ratios of the studied samples exhibit a good negative correlation with the F, indicating that the variations in partial melting producing the major element differences are generally coupled to the incompatible trace element abundances. We thus conclude that the excellent correlation between extents of melting and the Sr, Nd and Pb isotopic compositions can not be explained by melting of a uniform source.

PETROGENETIC MODEL

It should be stressed that the APR region is distant from any known hotspot; the closest is the Juan Fernandez hotspot, which lies approximately 3000 km north of the study area. If the enriched mantle is associated with higher potential temperatures by analogy with hotspots, higher upwelling temperatures should lead to greater degree of melting (e.g. Klein & Langmuir 1987). However, this is clearly not the case (Fig. 5f–i). The E-type basalts represent relatively low degree of melting relative to the N-type basalts, reflecting that the invasion of plume materials from deep mantle into the ambient N-type MORB mantle source can not be the source of the enriched materials beneath the APR. Therefore, it is considered that the subridge mantle is geochemically heterogeneous at a shallow level in the asthenosphere.

In Figure 6a,b, we show the Rb–Sr and Sm–Nd isotope data for the studied basalts. The correlation involving $^{147}Sm/^{144}Nd$ with $^{143}Nd/^{144}Nd$ is better than that involving $^{87}Rb/^{86}Sr$ with $^{87}Sr/^{86}Sr$. The scattering in the Rb–Sr systematics might be due to high mobility of Rb during low-temperature alteration processes, and the effects of variable crustal assimilation mentioned above. Clearly, the positive correlation observed in Sm–Nd

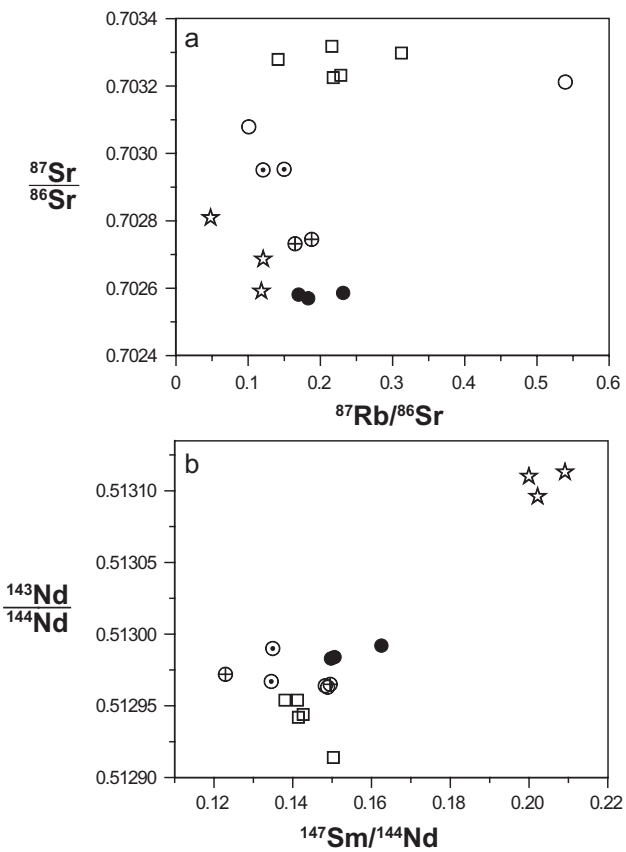

Fig. 6 (a) $^{87}Sr/^{86}Sr$ *vs* $^{87}Rb/^{86}Sr$, and (b) $^{143}Nd/^{144}Nd$ *vs* $^{147}Sm/^{144}Nd$ diagrams for the basalts from the Antarctic–Phoenix Ridge. Errors (2 σ) are within the size of the symbol on the plot. Symbols as in Figure 2.

systematics can not be a meaningful isochron because: (i) the slope of the pseudoisochron is defined by the positions of the two end-members (N- and E-type MORB) in the Sm–Nd space; and (ii) the two end-members are unlikely to have been comagmatic. Instead, the correlation might imply that both components are ancient and have developed their distinct isotopic characteristics independently for some time, regardless of the ultimate source of the enriched domains.

Basalts with elevated abundances of incompatible elements and enriched radiogenic isotopic characteristics, such as some of the APR samples, have been previously observed randomly from both axis and off-axis seamounts in the plume-absent East Pacific Rise (e.g. Batiza & Vanko 1984; Zindler *et al*. 1984; Graham *et al*. 1988; Hékinian *et al*. 1989; Niu *et al*. 1996) and in the Mid-Atlantic Ridge (Donnelly *et al*. 2004), indicating widespread existence of enriched domains in the ambient depleted mantle. It has been suggested that the enriched domains may represent remnants of ancient subducted oceanic crust or detached continental lithosphere, which survived in the convecting mantle (e.g. Zindler & Hart 1986; Niu *et al*. 1999). It is now a conventional view that the enriched heterogeneity may exist in the so-called 'marble cake' structure in the form of streaky, blob-riddled or veined mantle (e.g. Hanson 1977; Wood 1979; Allegrè & Turcotte 1986; Fitton & James 1986; Prinzhofer *et al*. 1989). In order to explain the close coexistence of distinct E-type MORB and N-type MORB in the APR, it seems reasonable to expect that the scale of heterogeneities is small. That is, the enriched component must exist in the form of highly localized spots or veins.

Shen and Forsyth (1995) argued that the final depth of melting, and possibly mean degree of melting, is likely to be controlled by loss of heat to the surface by conductive cooling during upwelling, which may be most visible at very slow spreading ridges. In the case where the upwelling rate decreases, the final depth of melting increases, resulting in decreasing average extent of melting. The subridge passive upwelling rate is proportional to the spreading rate. The apparent absence of extensive recent volcanic activity along this axial region of the APR, inferred from the very poorly defined central magnetic anomaly (e.g. Livermore *et al*. 2000), suggests that the final stage of volcanic activity, responsible for the E-type basalts, occurred prior to the magma supply shutting down following the extinction of the Antarctic–Phoenix Ridge (see above). It is thus reasonable to expect that the extent of melting decreases during the final stages of spreading since slower upwelling gives more time for the mantle to lose heat to the surface. Compared to the ambient depleted matrix, the enriched materials have high abundance of incompatible elements, and possibly high volatile contents (Aggrey *et al*. 1988; Michael 1995; Asimow & Langmuir 2003). The enriched component is thus the first fraction to enter the melt (e.g. Kushiro *et al*. 1968; Mysen & Boettcher 1975; Prinzhofer *et al*. 1989). This mechanism can explain the derivation of the E-type APR basalts representing relatively small extents of melt of the radiogenically enriched mantle source after the extinction of spreading in the APR. This interpretation is further substantiated by the observation that the E-type melts show a greater degree of fractionation, i.e. up to lower Mg# than the N-type basalts in this region (Fig. 3). In other words, it is possible that a correlation exists between extents of melting and subsequent crystal–melt fractionation because lower degree of melting creates smaller magma batches, which fractionate more extensively during ascent (Albarede & Tamagan 1988).

CONCLUSIONS

1. The E-type MORB coexists with the N-type MORB in the axial region of the Antarctic–Phoenix Ridge, which is far from any known hotspots.
2. The extent of enrichment in incompatible elements of the basalts correlates positively with isotopic ratios of Sr and Pb, and negatively with Nd.
3. The shallow level of the subridge mantle is compositionally heterogeneous.
4. The E-type melt compositions have been generated by low-degree partial melting of the enriched component in the heterogeneous mantle source after the extinction of spreading in the APR.
5. The enriched components in the ambient N-type MORB mantle source may exist in the form of highly localized spots or veins.

ACKNOWLEDGEMENTS

We are grateful to G. P. Yumul Jr, P. Castillo, and H. Bellon for their constructive reviews that greatly improved the original manuscript. We also thank the captain and crew of R/V *Yuzhmorgeologiya* for

their support during 2000–01 and 2002–03 summer cruises. This work was supported by the Korea Polar Research Institute (KOPRI) Project (PE07020; Formation, Evolution and Neotectonics of Antarctica).

REFERENCES

AGGREY K. E. D., MUENOW D. W. & BATIZA R. 1988. Volatile abundances in basaltic glasses from seamounts flanking the East Pacific Rise at 21°–14°N. *Geochimica et Cosmochimica Acta* **52**, 2115–9.

ALBAREDE F. & TAMAGAN V. 1988. Modeling the recent geochemical evolution of the Piton de la Fournaise Volcano, Reunion Island. *Journal of Petrology* **29**, 997–1030.

ALLEGRÈ C. J. & TURCOTTE D. L. 1986. Implications of a two-component marble-cake mantle. *Nature* **323**, 123–7.

ASIMOW P. D. & LANGMUIR C. H. 2003. The importance of water to oceanic mantle melting regimes. *Nature* **421**, 815–20.

BACH W., HEGNER E., ERZINGER J. & SATIR M. 1994. Chemical and isotopic variations along the superfast spreading East Pacific Rise from 6 to 30°S. *Contributions to Mineralogy and Petrology* **116**, 365–80.

BATIZA R. & VANKO D. A. 1984. Petrology of young Pacific seamounts. *Journal of Geophysical Research* **89**, 11 235–60.

CHAUVEL C. & BLICHERT-TOFT J. 2001. A hafnium isotope and trace element perspective on melting of the depleted mantle. *Earth and Planetary Science Letters* **190**, 137–51.

CHOE W. H., LEE J. I., LEE M. J., HUR S. D. & JIN Y. K. 2005. New approach on the extinction of spreading at the Phoenix Ridge, Antarctica. *Journal of the Petrological Society of Korea* **14**, 73–81 (in Korean with English abstract).

CHOE W. H., LEE J. I., LEE M. J., HUR S. D. & JIN Y. K. 2007. Origin of E-MORB in a fossil spreading center: The Antarctic-Phoenix Ridge, Drake Passage, Antarctica. *Geosciences Journal* **11**, 185–99.

DEBAILLE V., BLICHERT-TOFT J., AGRANIER A., DOUCELANCE R., SCHIANO P. & ALBAREDE F. 2006. Geochemical component relationships in MORB from the Mid-Atlantic Ridge, 22–35°N. *Earth and Planetary Science Letters* **241**, 844–62.

DONNELLY K. E., GOLDSTEIN S. L., LANGMUIR C. H. & SPIEGELMAN M. 2004. Origin of enriched ocean ridge basalts and implications for mantle dynamics. *Earth and Planetary Science Letters* **226**, 347–66.

DOSSO L., BOUGAULT H. & JORON J.-L. 1993. Geochemical morphology of the North Mid-Atlantic Ridges, 10°–24°N: Trace element-isotope complementary. *Earth and Planetary Science Letters* **120**, 443–62.

ELLAM R. M. 1992. Lithospheric thickness as a control on basalt geochemistry. *Geology* **20**, 153–6.

FITTON J. G. & JAMES D. 1986. Basic volcanism associated with intraplate linear features. *Philosophical Transactions of the Royal Society of London Series A* **317**, 253–66.

GRAHAM D. W., ZINDLER A., KURZ M. D., JENKINS W. J., BATIZA R. & STAUDIGEL H. 1988. He, Pb Sr, and Nd isotope constraints on magma genesis and mantle heterogeneity beneath young Pacific seamounts. *Contributions to Mineralogy and Petrology* **99**, 446–63.

HANSON G. N. 1977. Geochemical evolution of the suboceanic mantle. *Journal of Geological Society of London* **134**, 235–53.

HART S. R. 1984. A large-scale isotope anomaly in the southern hemisphere mantle. *Nature* **309**, 753–7.

HÉKINIAN R., THOMPSON G. & BIDEAU D. 1989. Axial and off-axial heterogeneity of basaltic rocks from the East Pacific Rise at 12°35′N–12°51′N and 11°26′N–11°30′N. *Journal of Geophysical Research* **94**, 17 437–63.

ITO E., WHITE W. M. & GÖPEL C. 1987. The O, Sr, Nd and Pb isotope geochemistry of MORB. *Chemical Geology* **62**, 157–76.

KLEIN E. M. & LANGMUIR C. H. 1987. Global correlations of ocean ridge basalt chemistry with axial depth and crustal thickness. *Journal of Geophysical Research* **92**, 8089–115.

KUSHIRO I., SYONO Y. & AKIMOTO S. 1968. Melting of a peridotite nodule at high pressures and high water pressures. *Journal of Geophysical Research* **73**, 6023–9.

LARTER R. D. & BARKER P. F. 1991. Effects of ridge crest trench interaction on Antarctic–Phoenix spreading—Forces on a young subducting plate. *Journal of Geophysical Research* **96**, 19 583–607.

LE ROEX A. P., DICK H. J. B. & WATKINS R. T. 1992. Petrogenesis of anomalous K-enriched MORB from the Southwest Indian Ridge: 11°53′E to 14°38′E. *Contributions to Mineralogy and Petrology* **110**, 253–68.

LIVERMORE R., BALANYÁ J. C., MALDONADO A. *et al.* 2000. Autopsy on a dead spreading center: The Phoenix Ridge, Drake Passage, Antarctica. *Geology* **28**, 607–10.

MAHONEY J. J., NATLAND J. H., POREDA W. R., BLOOMER S. H., FISHER R. L. & BAXTER A. N. 1989. Isotopic and geochemical provinces of the western Indian ocean spreading centers. *Journal of Geophysical Research* **94**, 4033–52.

MAHONEY J. J., LE ROEX A. P., PENG Z., FISHER R. L. & NATLAND J. H. 1992. Southwestern limits of Indian ocean ridge mantle and the origin of low $^{206}Pb/^{204}Pb$ mid-ocean ridge basalt: Isotope systematics of the central southwest Indian ridge (17°-50°E). *Journal of Geophysical Research* **97**, 19771–90.

MAHONEY J. J., SINTON J. M., KURZ M. D., MACDOUGALL J. D., SPENCER K. J. & LUGMAIR G. W. 1994.

Isotope and trace element characteristics of a superfast spreading ridge: East Pacific rise, 13–23°S. *Earth and Planetary Science Letters* **121**, 173–93.

MELSON W. G., VALLIER T. L., WRIGHT T. L., BYERLY G. & NELEN J. 1976. Chemical diversity of abyssal volcanic glass erupted along Pacific, Atlantic and Indian Ocean sea-floor spreading centers. *In* SUTTON, G. H., MANGHNANI, M. H. & MOBERLY, R. (eds). *The Geophysics of the Pacific Ocean and its Margin: A Volume in Honor of George P. Woollard.* Geophysical Monograph 19, pp. 351–68. American Geophysical Union, Washington.

MICHAEL P. J. 1995. Regionally distinctive sources of depleted MORB: Evidence from trace elements and H_2O. *Earth and Planetary Science Letters* **131**, 301–20.

MYSEN B. O. & BOETTCHER A. L. 1975. Melting of a hydrous mantle. II. Geochemistry of crystals and liquids formed by anatexis of mantle peridotite at high pressures and high temperatures as a function of controlled activities of water, hydrogen, and carbon dioxide. *Journal of Petrology* **16**, 549–93.

NIU Y. & BATIZA R. 1991. An empirical method for calculating melt compositions produced beneath mid-ocean ridges: Application for axis and off-axis (seamounts) melting. *Journal of Geophysical Research* **96**, 21 753–77.

NIU Y., WAGGONER D. G., SINTON J. M. & MAHONEY J. J. 1996. Mantle source heterogeneity and melting processes beneath seafloor spreading centers: The East Pacific Rise, 18°–19°S. *Journal of Geophysical Research* **101**, 27 711–33.

NIU Y., COLLERSON K. D., BATIZA R., WENDT J. I. & REGELOUS M. 1999. Origin of enriched-type mid-ocean ridge basalt at ridges far from mantle plumes: The East Pacific Rise at 11°20′N. *Journal of Geophysical Research* **104**, 7067–87.

PRINZHOFER A., LEWIN E. & ALLÈGRE C. J. 1989. Stochastic melting of the marble cake mantle: Evidence from local study of the East Pacific Rise at 12°50′N. *Earth and Planetary Science Letters* **92**, 189–206.

SALTERS V. J. M. & WHITE W. M. 1998. Hf isotope constraints on mantle evolution. *Chemical Geology* **145**, 447–60.

SCHILLING J.-G., ZAJAC M., EVANS R. *et al.* 1983. Petrological and geochemical variations along the Mid-Atlantic Ridge from 29°N to 73°N. *American Journal of Science* **283**, 510–86.

SHEN Y. & FORSYTH D. W. 1995. Geochemical constraints on initial and final depth of melting beneath mid-ocean ridges. *Journal of Geophysical Research* **100**, 2211–37.

SMITH W. H. F. & SANDWELL D. T. 1994. Bathymetric prediction from dense satellite altimetry and sparse shipboard bathymetry. *Journal of Geophysical Research* **99**, 21 803–24.

SUN S.-S. & MCDONOUGH W. F. 1989. Chemical and isotopic systematics of oceanic basalts: Implications for mantle composition and processes. *Geological Society of London* Spec. Publ. **42**, 313–45.

SUN S.-S., TATSUMOTO M. & SCHILLING J.-G. 1975. Mantle plume mixing along the Reykjanes ridge axis: Lead isotope evidence. *Science* **190**, 143–7.

TAYLOR R. N., THIRWALL M. F., MORTON B. J., HILTON D. R. & GEE M. A. M. 1997. Isotopic constraints on the influence of the Icelandic plume. *Earth and Planetary Science Letters* **148**, E1–8.

WHITE W. M. & HOFMANN A. W. 1982. Sr and Nd isotope geochemistry of oceanic basalts and mantle evolution. *Nature* **296**, 821–5.

WHITE W. M., HOFMANN A. W. & PUCHELT H. 1987. Isotope geochemistry of Pacific mid-ocean ridge basalt. *Journal of Geophysical Research* **92**, 4881–93.

WOOD D. A. 1979. A variably veined suboceanic upper mantle–genetic significance for mid-ocean ridge basalts from geochemical evidence. *Geology* **7**, 499–503.

ZINDLER A. & HART S. 1986. Chemical geodynamics. *Annual Review of Earth and Planetary Sciences* **14**, 493–571.

ZINDLER A., STAUDIGEL H. & BATIZA R. 1984. Isotope and trace element geochemistry of young Pacific seamounts: Implications for the scale of upper mantle heterogeneity. *Earth and Planetary Science Letters* **70**, 175–95.